A Simplified 3-D Constitutive Law for Magnetomechanical Behavior

Laurent Daniel[1,2], Olivier Hubert[3], and Mahmoud Rekik[3]

[1]Laboratoire de Génie Electrique de Paris (LGEP), CNRS(UMR 8507)/SUPELEC/
UPMC/Université Paris-Sud, 91192 Gif-sur-Yvette Cedex, France
[2]School of Materials, University of Manchester, Manchester M13 9PL, U.K.
[3]LMT-Cachan, ENS-Cachan/CNRS(UMR8535)/Université Paris Saclay, 94235 Cachan Cedex, France

The magnetomechanical behavior of magnetic materials is the result of intricate mechanisms at different scales. These mechanisms have been described with satisfying accuracy from micro-mechanical approaches. But, the corresponding constitutive laws would lead to prohibitive computation time if they were implemented in structural analysis tools for the design of electromagnetic devices. In this paper, a simplified approach for the modeling of multi-axial magnetoelastic behavior is proposed. This approach includes hysteresis effects and their dependence to stress. The corresponding very low computational time makes it suitable for an implementation into numerical tools for structural analysis.

Index Terms— **Hysteresis loops, magnetoelasticity, magnetostriction, multi-axial stress.**

I. Introduction

THE description of hysteresis in magnetic materials is a key to the design of electromagnetic devices. Among the available constitutive models for magnetic behavior, Preisach [1] and Jiles–Atherton [2] models stand as the most popular for the implementation into numerical analysis tools. Purely magnetic in their initial formulation, these models have been extended to account for the effect of coupled magnetomechanical loadings [3]–[7]. These extensions usually consider uniaxial stress configurations (pure tension or compression applied in a direction parallel to the magnetic field). But, in most practical devices, stress is multi-axial and its orientation with respect to the magnetic field can also be variable. This multi-axiality of magnetomechanical loadings can be handled in uniaxial models using the concept of equivalent stress [8], [9]. On the other hand, multi-scale approaches to multi-axial magnetoelastic behavior have been proposed [10]–[13] to describe the complex interactions between stress and magnetic field, as well as the significant anisotropy effects. They rely on an energetic description of the magnetomechanical equilibrium. However, their implementation into numerical design tools would lead to prohibitive computation times. Recently, some authors proposed multi-axial constitutive laws for magnetoelastic behavior together with a practical implementation into a finite-element formulation. Fonteyn *et al.* [14] proposed a thermodynamic approach based on a magnetomechanical definition of the Helmholtz free energy. Bernard *et al.* [15] used a simplified version of a previous multi-scale model [13] allowing its use in numerical analysis. Zeze *et al.* [16] used a phenomenological approach derived from the so-called E&S model [17]. Only the latter includes hysteresis effects, the first two being anhysteretic models. In this paper, we propose to include hysteresis effects in the simplified approach proposed in [15] by taking benefit of a recent extension of the multi-scale approach to hysteretic behavior [18]. In a first part, this hysteretic magnetomechanical constitutive law is detailed. The identification of the material parameters is then discussed. Modeling results are finally compared with experimental measurements obtained from non oriented iron-silicon steel.

Manuscript received May 24, 2014; revised July 28, 2014 and August 26, 2014; accepted September 30, 2014. Date of current version April 22, 2015. Corresponding author: L. Daniel (e-mail: laurent.daniel@supelec.fr).

Color versions of one or more of the figures in this paper are available online at http://ieeexplore.ieee.org.

Digital Object Identifier 10.1109/TMAG.2014.2361643

II. Constitutive Law

The proposed simplified approach to define the constitutive magnetomechanical behavior of magnetic materials is derived in two steps. The anhysteretic behavior is calculated first from a simplification of a previous multi-scale model [12], [13]. This simplified approach was proposed initially for 2-D problems [15] and then extended to 3-D problems [19]. The 3-D version is used here. In a second step, the hysteresis effects are added by introducing a supplementary magnetic field according to the recent extension [18] of the multi-scale model. The definition of this constitutive law is detailed hereafter.

In contrast with the full multi-scale model [18], the polycrystalline material is described as a fictitious single crystal with a very large number of easy magnetization directions. The material is hence described as a collection of magnetic domains randomly oriented. The specific properties of the fictitious single crystal are identified from the macroscopic behavior. The reversible (anhysteretic) part of the magnetomechanical behavior is calculated first [19]. The local free energy of the material (1) is written at the domain scale (α) and defined as the sum of three contributions. The magnetostatic (Zeeman) energy (2) tends to align the local magnetization $\mathbf{M}_\alpha$ with the applied field $\mathbf{H}$. μ_0 is the vacuum permeability. The magnetoelastic energy (3) describes the effect of the applied stress $\boldsymbol{\sigma}$ on the behavior. It introduces the local magnetostriction strain $\boldsymbol{\varepsilon}_\alpha^\mu$. An anisotropy energy (4) can be added to describe macroscopic anisotropy effects, for example, resulting from the combination of crystalline anisotropy and crystallographic texture. It is given here for a uniaxial anisotropy along direction $\boldsymbol{\beta}$, J being a constant to be identified. If we assume macroscopic isotropy, this

term vanishes

$$W_\alpha = W_\alpha^{\text{mag}} + W_\alpha^{el} + W_\alpha^{an} \quad (1)$$

$$W_\alpha^{\text{mag}} = -\mu_0 \, \mathbf{H}.\mathbf{M}_\alpha \quad (2)$$

$$W_\alpha^{el} = -\boldsymbol{\sigma} : \boldsymbol{\varepsilon}_\alpha^{\mu} \quad (3)$$

$$W_\alpha^{an} = J(\boldsymbol{\alpha}.\boldsymbol{\beta})^2. \quad (4)$$

The local magnetization $\mathbf{M}_\alpha$ (5) is given by its direction $\boldsymbol{\alpha}$ (unit vector), and its norm is the saturation magnetization M_s of the material. Assuming an isotropic and isochoric magnetostriction behavior, the magnetostriction strain $\boldsymbol{\varepsilon}_\alpha^{\mu}$ is given by (6). λ_s is the saturation magnetostriction of the material. The anisotropy of the macroscopic magnetostriction can be considered to the price of additional material parameters (see for instance [15])

$$\mathbf{M}_\alpha = M_s \, \boldsymbol{\alpha} \quad (5)$$

$$\boldsymbol{\varepsilon}_\alpha^{\mu} = \lambda_s \left(\frac{3}{2} \, \boldsymbol{\alpha} \otimes \boldsymbol{\alpha} - \frac{1}{2} \, \mathbf{I} \right). \quad (6)$$

The volume fraction f_α of domains with orientation $\boldsymbol{\alpha}$ (7) is then defined as an internal variable. It is defined with a Boltzmann probability function [10]. A_s (8) is a material parameter linked to the initial anhysteretic susceptibility χ^o [12]

$$f_\alpha = \frac{\exp\left(-A_s W_\alpha\right)}{\displaystyle\int_\alpha \exp(-A_s W_\alpha)} \quad (7)$$

$$A_s = \frac{3 \, \chi^o}{\mu_0 \, M_s^2}. \quad (8)$$

Once the volume fraction f_α is defined, the macroscopic magnetization $\mathbf{M}$ (9) and magnetostriction $\boldsymbol{\varepsilon}^{\mu}$ (10) are obtained through averaging operations over all possible directions for the magnetization direction $\boldsymbol{\alpha}$

$$\mathbf{M} = \langle \mathbf{M}_\alpha \rangle = \int_\alpha f_\alpha \, \mathbf{M}_\alpha \quad (9)$$

$$\boldsymbol{\varepsilon}^{\mu} = \langle \boldsymbol{\varepsilon}_\alpha^{\mu} \rangle = \int_\alpha f_\alpha \, \boldsymbol{\varepsilon}_\alpha^{\mu}. \quad (10)$$

This integration step can be performed numerically using a discretization of a unit sphere for the possible orientations $\boldsymbol{\alpha}$ [13].

To describe the effect of stress on the initial domain structure, a configuration field $\mathbf{H}^\sigma$ (11) is added to the anhysteretic field $\mathbf{H}$ [18]

$$\mathbf{H}^\sigma = \eta \left(N^\sigma - \frac{1}{3} \right) \mathbf{M} \quad (11)$$

where η is a material parameter. N^σ (12) belongs to the interval [0, 1] and is $1/3$ when no stress is applied. K (13) is defined as a function of A_s and λ_s. σ^{eq} is the equivalent stress for $\boldsymbol{\sigma}$ as defined in [20], namely the projection along the magnetic field direction of the deviatoric part of $\boldsymbol{\sigma}$. $\mathbf{h}$ (unit vector) is the direction of the magnetic field $\mathbf{H}$

$$N^\sigma = \frac{1}{1 + 2 \exp\left(-K \, \sigma^{\text{eq}}\right)} \quad (12)$$

$$K = \frac{3}{2} \, A_s \, \lambda_s \quad (13)$$

$$\sigma^{\text{eq}} = \frac{3}{2} \, \mathbf{h} \, . \left(\boldsymbol{\sigma} - \frac{1}{3} \text{tr}(\boldsymbol{\sigma}) \, \mathbf{I} \right) . \, \mathbf{h}. \quad (14)$$

This configuration field notably allows the description of the non-monotonic effect of stress on the magnetic permeability observed in some materials [18].

Hysteresis effects are introduced in the model by adding an irreversible contribution $\mathbf{H}_{\text{irr}}$ to the anhysteretic magnetic field. The definition of $\mathbf{H}_{\text{irr}}$ is based on the works of Hauser [21], extended to magnetomechanical loadings. $\mathbf{H}_{\text{irr}}$ is assumed to be parallel to the increment of $\mathbf{H}$. This is a strong assumption, and significant limitations are expected for some magnetic loadings, particularly rotational loadings. The norm of $\mathbf{H}_{\text{irr}}$ is given by (15)

$$||\mathbf{H}_{\text{irr}}|| = \delta \left(\frac{k_r}{\mu_0 M_s} + c_r ||\mathbf{H}|| \right) \times \left[1 - \kappa \, \exp\left(- \frac{k_a}{\kappa} \, ||\mathbf{M} - \mathbf{M}^{\text{inv}}|| \right) \right] \quad (15)$$

where δ is equal to ± 1, depending on whether the material is being loaded or unloaded. The sign of δ is changed each time when there is an inversion in the loading direction. k_r, c_r, k_a, and κ are material parameters. The value of κ changes each time when there is an inversion in the loading direction [21]. The new value κ is calculated from the previous value κ^o according to (16). The initial value κ^{ini} of κ is a material constant. $\mathbf{M}^{\text{inv}}$ is the value of $\mathbf{M}$ at the previous inversion of the loading direction [18]

$$\kappa = 2 - \kappa^o \, \exp\left(- \frac{k_a}{\kappa^o} \, ||\mathbf{M} - \mathbf{M}^{\text{inv}}|| \right). \quad (16)$$

To account for the dependence of the coercive field to the applied stress, the parameter k_r (17), defining the coercive field, is assumed to show a dependence to stress similar to the stress configuration effect, k_r^0 being a material constant [18]

$$k_r = k_r^0 \left(\frac{4}{3} - N^\sigma \right). \quad (17)$$

A more precise description of the effect of stress on the coercive field can be obtained using an adjustment parameter ζ, similar to η for the configuration field $\mathbf{H}^\sigma$ (11). Equation (17) is then transformed into (18). This parameter ζ has not been used here ($\zeta = 1$)

$$k_r = k_r^0 \left(1 - \zeta \left(N^\sigma - \frac{1}{3} \right) \right). \quad (18)$$

Once the macroscopic magnetization $\mathbf{M}$ and magnetostriction $\boldsymbol{\varepsilon}^{\mu}$ are calculated as a function of the anhysteretic field $\mathbf{H}$ and stress tensor $\boldsymbol{\sigma}$, the effective magnetic field $\tilde{\mathbf{H}}$ (19) is calculated by adding the configuration field $\mathbf{H}^\sigma$ and the hysteresis contribution $\mathbf{H}_{\text{irr}}$ to the anhysteretic field

$$\tilde{\mathbf{H}} = \mathbf{H} + \mathbf{H}^\sigma + \mathbf{H}_{\text{irr}}. \quad (19)$$

This simplified approach allows the reduction of the computational cost by a factor higher than 1000 compared with the full multi-scale approach [18].

III. Identification of Model Parameters

The modeling parameters can be separated into two sets: 1) anhysteretic and 2) hysteretic material parameters. Four parameters are used to describe the anhysteretic behavior. M_s is the saturation magnetization and λ_s is the saturation

TABLE I
MATERIAL PARAMETERS: ANHYSTERETIC PART

Parameter	M_s	λ_s	A_s	η
Value	$1.45\ 10^6$	12	$3.5\,10^{-3}$	$2\,10^{-4}$
Unit	A/m	10^{-6}	m^3/J	-

TABLE II
MATERIAL PARAMETERS: HYSTERETIC PART

Parameter	k_r^0	c_r	k_a	κ^{ini}
Value	150	0.1	$19\,10^{-6}$	1
Unit	J/m^3	-	m/A	-

magnetostriction strain. It was found, however, that the model shows better accuracy if rather than the standard physical values, M_s and λ_s are taken as the maximum magnetization and strain, respectively. These values can be identified from a macroscopic measurement in the absence of applied stress. The parameter A_s is proportional to the initial slope of the unstressed anhysteretic magnetization curve (8). It can then be identified from a low-field anhysteretic measurement under no applied stress. η describes the non-monotonic effect of stress on the magnetic behavior. It can be identified from a susceptibility measurement under stress. The sensitivity to stress being much higher at low field, it is suggested to perform the identification of η from low-field anhysteretic measurements under uniaxial stress. Tension configurations should usually be sufficient for the purpose of this identification. The anhysteretic parameters are summarized in Table I indicating the values used in this paper.

Four parameters are also required to describe the hysteretic part of the behavior according to Hauser's approach [21]. They can be chosen so as to adjust the description of a major magnetization loop under no applied stress starting from a demagnetized state. k_r^0 controls the coercive field amplitude, c_r the first magnetization behavior, and k_a and κ^{ini} the inclination of the hysteresis cycle and the approach to saturation. The values used in this paper are summarized in Table II.

In summary, the material parameters can be obtained from one anhysteretic magnetization and magnetostriction measurement at high field (or two orthogonal magnetostriction measurements in the case of anisotropic materials), from anhyteretic measurements at low field under uniaxial stress (tension) and from a major hysteresis loop under no applied stress. After this identification from 1-D measurements, the model can be used to predict the material response under any magnetoelastic loading, including multi-axial configurations. Comparison to experimental results are proposed in Section IV.

IV. HYSTERESIS LOOPS AND HYSTERESIS LOSSES

The proposed simplified model enables a very fast evaluation of hysteresis loops under stress. Fig. 1(a) gives an example of magnetization curves for a nonoriented iron-silicon alloy subjected to a uniaxial compression applied in the direction parallel to the magnetic field. It shows a decrease of magnetic induction under compressive stress, with hysteresis loops becoming more and more inclined

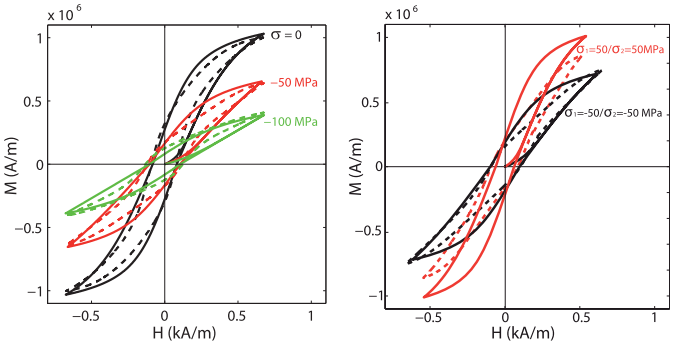

Fig. 1. Magnetization curves for $f = 5$ Hz under stress. Dashed lines: experimental results. Plain lines: numerical results. The magnetic field is applied along the stress direction for uniaxial loading and along direction 1 for biaxial loadings. (a) Uniaxial stress. (b) Equibiaxial stress.

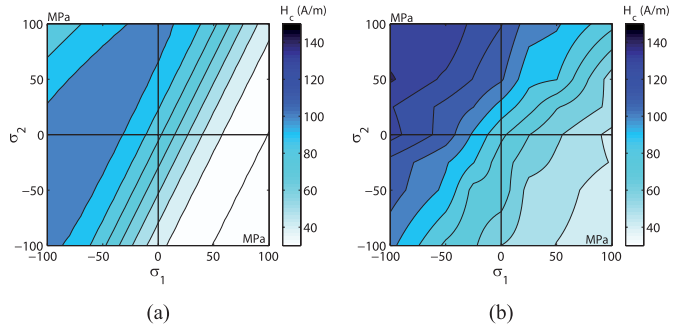

Fig. 2. Coercive field under biaxial stress. Results for a maximum magnetic field $H_{\text{max}} = 650$ A/m applied along direction 1. (a) Modeling results. (b) Experimental results.

toward the horizontal axis, as already observed previously in stainless steel [22]. The model can also be used to predict the behavior of the material under multi-axial configuration. Fig. 1(b) shows the hysteresis loops under equibiaxial mechanical loading. Equibitraction slightly enhances the magnetic behavior, while a strong degradation is observed under equibicompression. The modeling results tend to overestimate the effect of stress. The experimental results are part of an experimental characterization campaign presented in [23]. The model does not reproduce exactly the shape of the experimental hysteresis loops, but the effect of stress is correctly described.

The model can also be used to predict the behavior of the material under more general multi-axial configuration. As an example, the evolution of the coercive field under biaxial loading is shown in Fig. 2(a). The stress is a static biaxial stress (σ_1, σ_2) and the magnetic field is applied along direction 1 with a maximum amplitude of 650 A/m. It must be noticed that hysteresis loops in this case are not major loops. The corresponding experimental results [23] are shown in Fig. 2(b).

The modeling results show similar trends as the experimental measurements. The coercive field is decreasing with the component of the stress tensor σ_1 aligned with the magnetic field, and increasing with the perpendicular component σ_2. The order of magnitude for the coercive field is correct although the effect of stress is underestimated in the second quadrant $(\sigma_1 < 0,\ \sigma_2 > 0)$, and overestimated in the fourth quadrant $(\sigma_1 > 0,\ \sigma_2 < 0)$. The isovalues for the coercive field are

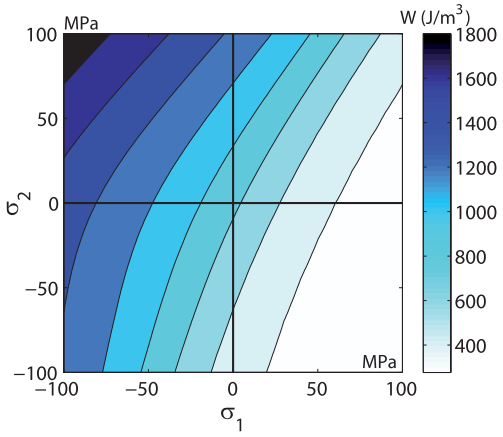

Fig. 3. Hysteresis losses under biaxial stress. Major loops: modeling results.

approximately parallel lines with a slightly higher slope obtained from the model compared with the measurements. In the second quadrant, for high level of shear stress, the model predicts an inversion of the variation for the coercive field that is not observed experimentally for this material.

Hysteresis losses as a function of stress can also be estimated. Fig. 3 shows the losses obtained under biaxial loading. For this figure, the losses have been calculated on major loops. In that, case saturation is reached and the maximum applied field is much higher than 650 A/m. The results obtained under uniaxial tension (axis $\sigma_2 = 0$) are consistent with previous measurements [24] showing an increase of losses under compression and a decrease with moderate magnitude in tension.

Due to the strong simplifications made, the proposed model is expected to be less accurate than the full multi-scale approach but the comparison with experimental results obtained under biaxial magnetomechanical loading shows satisfying agreement. The approach gives a reasonable estimate of the effect of stress on both magnetization and hysteresis losses in magnetic materials subjected to multi-axial magnetomechanical loadings. The computation cost is low enough to allow an implementation into a numerical analysis software.

V. Conclusion

A model for the behavior of magnetic materials under multi-axial stress is proposed. This model includes hysteresis effects. It is derived from the simplification of a multi-scale approach based on an energetic description at the magnetic domain scale [18]. The model has been validated for 2-D magnetomechanical loadings consisting of biaxial stress combined with 1-D in-plane magnetic field. The application to more complex configurations, including rotational magnetic field is a further objective. The compactness of this simplified approach allows its practical implementation into finite element tools for the design of electromagnetic devices.

References

[1] F. Preisach, "Über die magnetische Nachwirkung," *Zeitschrift Phys.*, vol. 94, nos. 5–6, pp. 277–302, 1935.

[2] D. C. Jiles and D. L. Atherton, "Theory of ferromagnetic hysteresis (invited)," *J. Appl. Phys.*, vol. 55, no. 6, pp. 2115–2120, Mar. 1984.

[3] A. Bergqvist and G. Engdahl, "A stress-dependent magnetic Preisach hysteresis model," *IEEE Trans. Magn.*, vol. 27, no. 6, pp. 4796–4798, Nov. 1991.

[4] M. J. Sablik and D. C. Jiles, "Coupled magnetoelastic theory of magnetic and magnetostrictive hysteresis," *IEEE Trans. Magn.*, vol. 29, no. 5, pp. 2113–2123, Jul. 1993.

[5] A. A. Adly and I. D. Mayergoyz, "Magnetostriction simulation using anisotropic vector Preisach-type models," *IEEE Trans. Magn.*, vol. 32, no. 5, pp. 4773–4775, Sep. 1996.

[6] O. Bottauscio, A. Lovisolo, P. E. Roccato, M. Zucca, C. Sasso, and R. Bonin, "Modeling and experimental analysis of magnetostrictive devices: From the material characterization to their dynamic behavior," *IEEE Trans. Magn.*, vol. 44, no. 11, pp. 3009–3012, Nov. 2008.

[7] J. Li and M. Xu, "Modified Jiles-Atherton-Sablik model for asymmetry in magnetomechanical effect under tensile and compressive stress," *J. Appl. Phys.*, vol. 110, no. 6, pp. 063918-1–063918-4, Sep. 2011.

[8] G. Krebs and L. Daniel, "Giant magnetostrictive materials for field weakening: A modeling approach," *IEEE Trans. Magn.*, vol. 48, no. 9, pp. 2488–2494, Sep. 2012.

[9] K. Yamazaki and Y. Kato, "Iron loss analysis of interior permanent magnet synchronous motors by considering mechanical stress and deformation of stators and rotors," *IEEE Trans. Magn.*, vol. 50, no. 2, Feb. 2014, Art. ID 7022504.

[10] N. Buiron, L. Hirsinger, and R. Billardon, "A multiscale model for magneto-elastic couplings," *J. Phys. IV France*, vol. 9, no. PR9, pp. Pr9-187–Pr9-196, Sep. 1999.

[11] W. D. Armstrong, "A directional magnetization potential based model of magnetoelastic hysteresis," *J. Appl. Phys.*, vol. 91, no. 4, pp. 2202–2210, 2002.

[12] L. Daniel, O. Hubert, N. Buiron, and R. Billardon, "Reversible magneto-elastic behavior: A multiscale approach," *J. Mech. Phys. Solids*, vol. 56, no. 3, pp. 1018–1042, Mar. 2008.

[13] L. Daniel and N. Galopin, "A constitutive law for magnetostrictive materials and its application to Terfenol-D single and polycrystals," *Eur. Phys. J. Appl. Phys.*, vol. 42, no. 2, pp. 153–159, May 2008.

[14] K. Fonteyn, A. Belahcen, R. Kouhia, P. Rasilo, and A. Arkkio, "FEM for directly coupled magneto-mechanical phenomena in electrical machines," *IEEE Trans. Magn.*, vol. 46, no. 8, pp. 2923–2926, Aug. 2010.

[15] L. Bernard, X. Mininger, L. Daniel, G. Krebs, F. Bouillault, and M. Gabsi, "Effect of stress on switched reluctance motors: A magneto-elastic finite-element approach based on multiscale constitutive laws," *IEEE Trans. Magn.*, vol. 47, no. 9, pp. 2171–2178, Sep. 2011.

[16] S. Zeze, Y. Kai, T. Todaka, and M. Enokizono, "Vector magnetic characteristic analysis of a PM motor considering residual stress distribution with complex-approximated material modeling," *IEEE Trans. Magn.*, vol. 48, no. 11, pp. 3352–3355, Nov. 2012.

[17] M. Enokizono and Y. Fujita, "Improvement of E&S modeling for eddy-current magnetic field analysis," *IEEE Trans. Magn.*, vol. 38, no. 2, pp. 881–884, Mar. 2002.

[18] L. Daniel, M. Rekik, and O. Hubert, "A multiscale model for magneto-elastic behaviour including hysteresis effects," *Arch. Appl. Mech.*, vol. 84, no. 9, pp. 1307–1323, Oct. 2014.

[19] L. Daniel, "An analytical model for the effect of multiaxial stress on the magnetic susceptibility of ferromagnetic materials," *IEEE Trans. Magn.*, vol. 49, no. 5, pp. 2037–2040, May 2013.

[20] L. Daniel and O. Hubert, "An equivalent stress for the influence of multiaxial stress on the magnetic behavior," *J. Appl. Phys.*, vol. 105, no. 7, pp. 07A313-1–07A313-3, Apr. 2009.

[21] H. Hauser, "Energetic model of ferromagnetic hysteresis: Isotropic magnetization," *J. Appl. Phys.*, vol. 96, no. 5, pp. 2753–2767, Sep. 2004.

[22] H. Kwun and G. L. Burkhardt, "Effects of grain size, hardness, and stress on the magnetic hysteresis loops of ferromagnetic steels," *J. Appl. Phys.*, vol. 61, no. 4, pp. 1576–1579, 1987.

[23] M. Rekik, O. Hubert, and L. Daniel, "Influence of a multiaxial stress on the reversible and irreversible magnetic behaviour of a 3%Si-Fe alloy," *Int. J. Appl. Electromagn. Mech.*, vol. 44, nos. 3–4, pp. 301–315, Mar. 2014.

[24] M. LoBue, V. Basso, F. Fiorillo, and G. Bertotti, "Effect of tensile and compressive stress on dynamic loop shapes and power losses of Fe-Si electrical steels," *J. Magn. Magn. Mater.*, vols. 196–197, pp. 372–374, May 1999.